

# Flow Rate Optimization for the Quadrupole Magnetic Cell Sorter

P. Stephen Williams,<sup>\*,†</sup> Maciej Zborowski,<sup>‡</sup> and Jeffrey J. Chalmers<sup>§</sup>

Department of Chemistry and Geochemistry, Colorado School of Mines, 1500 Illinois Street, Golden, Colorado 80401, Department of Biomedical Engineering, The Cleveland Clinic Foundation, 9500 Euclid Avenue, Cleveland, Ohio 44195, and Department of Chemical Engineering, The Ohio State University, 140 West 19th Avenue, Columbus, Ohio 43210

**The quadrupole magnetic cell sorter is a form of split-flow thin-channel (SPLITT) separation device. It employs a quadrupole magnetic field and annular channel geometry. Immunomagnetic labels are used to bind to specific receptors on the surface of the cells of interest. It is the interaction of these labels with the magnetic field that brings about the selective isolation of these cells. The SPLITT separation devices have generally been based on parallel-plate geometry, usually with effectively constant field strength applied across the channel thickness. The nonconstant field strength and annular channel geometry of the magnetic cell sorter require that a new strategy be developed for optimization of inlet and outlet flow rates. We present such a strategy here based on a consideration of certain specific cell trajectories within the system.**

Split-flow thin-channel (SPLITT) separation cells allow for the rapid and continuous separation of suspended materials (particles or macromolecules).<sup>1–3</sup> The separation is usually of a binary nature, although higher order separations are possible. (Continuous separation into more than two subpopulations is more easily accomplished by linking SPLITT cells in series.<sup>1,4</sup>) The separation takes place within the laminar flow of a carrier fluid along a thin channel. A field or gradient is imposed across the thin dimension of the channel, perpendicular to the direction of flow. The sample mixture is arranged to enter the system close to one of the channel walls as a thin stream lamina. This is achieved by merging flow from each side of a thin stream splitter placed midway across the channel thickness, inside the inlet end of the channel. As they are carried along the channel by the flow of fluid, those components that interact more strongly with the field or gradient are carried transversely across the channel thickness to a greater extent than those that interact only weakly. A division of flow at the channel outlet using a second stream splitter then completes the separation of the sample into two fractions.

Many different fields and gradients may be employed, depending on the nature of the sample. A simple gravitational or centrifugal field separates material according to its sedimentation coefficient.<sup>2,4–7</sup> Electrical fields have been used to separate charged species.<sup>8,9</sup> Hydrodynamic lift forces generated by the flow of carrier fluid have been used to separate species according, principally, to size.<sup>10,11</sup> The diffusion rates of components from the region of higher concentration near the wall, where the sample is introduced, across the channel to regions of lower concentration have also been exploited.<sup>12,13</sup>

More recently, magnetic fields were used to separate and purify biological materials used in various areas of biotechnology and cellular therapy.<sup>14–18</sup> Perhaps the technique holds its greatest potential in the isolation and purification of specific cell types. The key to carrying out these selective separations is the use of immunomagnetic labeling. The immunomagnetic labels are composed of a paramagnetic component bound to an antibody, which interacts with and binds to a specific cell surface marker. The most successful separations have employed labels composed of magnetite of colloidal dimensions coated with dextran,<sup>14–19</sup> although larger beads and molecular (ferritin) labels<sup>19</sup> have also been considered.

<sup>†</sup> Colorado School of Mines. E-mail: pswillia@mines.edu. Fax: (303) 273-3629.

<sup>‡</sup> The Cleveland Clinic Foundation. E-mail: zborow@bme.ri.ccf.org. Fax: (216) 444-9198.

<sup>§</sup> The Ohio State University. E-mail: chalmers.1@osu.edu. Fax: (614) 292-3769.

- (1) Giddings, J. C. *Sep. Sci. Technol.* **1985**, *20*, 749–768.
- (2) Springston, S. R.; Myers, M. N.; Giddings, J. C. *Anal. Chem.* **1987**, *59*, 344–350.
- (3) Giddings, J. C. *Sep. Sci. Technol.* **1988**, *23*, 931–943.
- (4) Gao, Y.; Myers, M. N.; Barman, B. N.; Giddings, J. C. *Part. Sci. Technol.* **1991**, *9*, 105–118.

- (5) Fuh, C. B.; Myers, M. N.; Giddings, J. C. *Anal. Chem.* **1992**, *64*, 3125–3132.
- (6) Fuh, C. B.; Myers, M. N.; Giddings, J. C. *Ind. Eng. Chem. Res.* **1994**, *33*, 355–362.
- (7) Fuh, C. B.; Giddings, J. C. *Biotechnol. Prog.* **1995**, *11*, 14–20.
- (8) Giddings, J. C. *J. Chromatogr.* **1989**, *480*, 21–33.
- (9) Levin, S.; Myers, M. N.; Giddings, J. C. *Sep. Sci. Technol.* **1989**, *24*, 1245–1259.
- (10) Giddings, J. C. *Sep. Sci. Technol.* **1988**, *23*, 119–131.
- (11) Zhang, J.; Williams, P. S.; Myers, M. N.; Giddings, J. C. *Sep. Sci. Technol.* **1994**, *29*, 2493–2522.
- (12) Williams, P. S.; Levin, S.; Lenczycki, T.; Giddings, J. C. *Ind. Eng. Chem. Res.* **1992**, *31*, 2172–2181.
- (13) Levin, S.; Giddings, J. C. *J. Chem. Technol. Biotechnol.* **1991**, *50*, 43–56.
- (14) Zborowski, M.; Williams, P. S.; Sun, L.; Moore, L. R.; Chalmers, J. J. *J. Liq. Chromatogr. Relat. Technol.* **1997**, *20*, 2887–2905.
- (15) Chalmers, J. J.; Zborowski, M.; Sun, L.; Moore, L. *Biotechnol. Prog.* **1998**, *14*, 141–148.
- (16) Sun, L.; Zborowski, M.; Moore, L. R.; Chalmers, J. J. *Cytometry* **1998**, *33*, 469–475.
- (17) Zborowski, M.; Sun, L.; Moore, L. R.; Williams, P. S.; Chalmers, J. J. *Magn. Mater.* **1999**, *194*, 224–230.
- (18) Zborowski, M.; Sun, L.; Moore, L. R.; Chalmers, J. J. *ASAIO J.*, in press.
- (19) Zborowski, M.; Moore, L. R.; Sun, L.; Chalmers, J. J. In *Scientific and Clinical Applications of Magnetic Microcarriers: An Overview*; Häfeli, U., Schütt, W., Teller, J., Zborowski, M., Eds.; Plenum Press: New York, 1997; pp 247–260.

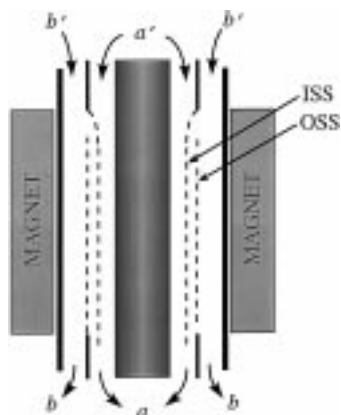


Figure 1. Cross section of quadrupole magnetic cell sorter. The radius has been expanded for clarity. The cell sample is fed in at  $a'$ , and carrier fluid, at  $b'$ . The inlet splitting surface (ISS) corresponds to the inner broken lines, and the outlet splitting surface (OSS), to the outer broken lines. Sorted fractions are collected at outlets  $a$  and  $b$ .

The magnetic system employs a quadrupole magnetic field and an annular SPLITT geometry. The quadrupole field results in a magnetic energy gradient that increases linearly with distance from the axis of symmetry and is independent of both radial direction and distance along the length of the system (except for some perturbations near the ends of the system). The SPLITT systems have generally been based on a parallel-plate geometry, but an annular geometry lends itself to the quadrupole magnetic field. To make use of the tendency for labeled cells to migrate away from the axis of the system toward the outer wall, the sample must be introduced close to the inner wall of the annulus. The system is shown in cross section in Figure 1, where the radial dimension has been expanded for clarity. The flow splitters for the annular system are cylindrical and must be accurately placed concentrically with the walls of the annulus. The positions of the virtual surfaces that fall between the fluid streamlines that enter at inlets  $a$  and  $a'$  (the inlet splitting surface, ISS) and between streamlines that exit at outlets  $b$  and  $b'$  (the outlet splitting surface, OSS) are shown as dashed lines. There is no inherent disadvantage associated with the annular SPLITT geometry. In fact, this geometry does not suffer from the edge perturbations associated with the parallel-plate geometry. The increase of circumference with radial distance from the axis of symmetry, however, must be taken into account when positions of the ISS and OSS are calculated. The fluid velocity profile across the thickness of the annulus must also be incorporated into the theoretical treatment of the system, in addition to the increasing magnetic force experienced by the cells and their consequent increasing radial velocities as they migrate toward the outer wall. The theoretical treatment of the system is therefore more complicated than that of the parallel-plate SPLITT systems. Once the required flow rates for the two inlets and two outlets have been determined, the operation of the system should be as straightforward as that of other SPLITT systems. The quadrupole magnetic cell sorter also has the advantage of containing no moving parts and has no dependence on a power supply when permanent magnets are used. We present our approach to determining required flow rates below.

## THEORY

It may be shown<sup>20</sup> that a paramagnetic particle of volume  $V_m$ , placed in a magnetic field, experiences a force  $F_m$  given by

$$F_m = V_m \Delta\chi \frac{|\nabla B^2|}{2\mu_0} \quad (1)$$

where  $\Delta\chi$  is the magnetic susceptibility of the particle relative to that of the suspending medium,  $B$  is the magnetic field intensity, and  $\mu_0$  is the magnetic permeability of free space. This relationship may be written in the form

$$F_m = \phi_m S_m \quad (2)$$

in which  $S_m$  is a measure of magnetic field strength, given by

$$S_m = \frac{|\nabla B^2|}{2\mu_0} \quad (3)$$

and  $\phi_m$  is the particle-magnetic field interaction parameter, given by

$$\phi_m = V_m \Delta\chi \quad (4)$$

When the particle is suspended in a viscous fluid, it quickly attains a velocity  $u_m$  at which the force due to interaction with the magnetic field is exactly opposed by the drag of the fluid. This velocity is given by

$$u_m = F_m/f \quad (5)$$

where  $f$  is the particle friction coefficient, equal to  $3\pi\eta d$  for a spherical particle of diameter  $d$ , with  $\eta$  being the viscosity of the suspending fluid. It follows that

$$u_m = \frac{\phi_m}{f} S_m = m_m S_m \quad (6)$$

in which  $m_m$  is the magnetophoretic mobility of the particle, equal to  $\phi_m/f$ .

In our system, the magnetic field interacts not directly with a biological cell to any significant extent but with the immunomagnetic labels attached to its surface. The force acting on the cell  $F_m$  is simply the sum of the forces  $\phi_l$  acting on the individual magnetic labels. Therefore we have<sup>15</sup>

$$F_m = A_c \alpha \beta F_l \quad (7)$$

where  $A_c$  is the surface area of the cell,  $\alpha$  is the number of markers per unit area of the cell surface, and  $\beta$  is the number of labels attached to each marker. It is of course assumed that the cell is sufficiently small that the field strength does not vary significantly across its surface. It follows that

(20) Zborowski, M. In *Scientific and Clinical Applications of Magnetic Microcarriers: An Overview*; Häfeli, U., Schütt, W., Teller, J., Zborowski, M., Eds.; Plenum Press: New York, 1997; pp 205–231.

$$\phi_m = A_c \alpha \beta \phi_1 \quad (8)$$

where  $\phi_m$  and  $\phi_1$  are the particle-field interaction parameters for the labeled cell and for an individual label, respectively. Hence, for a spherical cell (for which  $A_c = \pi a^2$ ), we have

$$m_m = \frac{\phi_m}{f} = \frac{d\alpha\beta\phi_1}{3\eta} \quad (9)$$

where  $m_m$  is the magnetophoretic mobility of the cell.

In the theoretical treatment of the system developed below, we shall assume that  $\phi_1$  is constant for the range of field strength in the quadrupole system. In other words, it will be assumed that magnetic saturation effects are not exhibited. A labeled cell will therefore be expected to exhibit constant  $m_m$  within the system. The magnetic mobility of a labeled cell is obtained by measuring the field-induced velocity under a known magnetic field strength.<sup>21,22</sup> It is given simply by a rearrangement of eq 6

$$m_m = u_m / S_m \quad (10)$$

and once this is known, the cell velocity will be known for any other field strength, provided  $\phi_1$  and hence  $m_m$  remain constant with field strength.

For the quadrupole magnetic field we have<sup>23</sup>

$$S_m = \frac{B_o^2}{\mu_o r_o^2} r = \frac{B_o^2}{\mu_o r_o} \rho \quad (11)$$

where  $B_o$  is the magnetic field intensity at the inner surface of the outer wall,  $r_o$  is the radius of this inner surface,  $r$  is the radial distance from the axis, and  $\rho = r/r_o$ . We may write this as

$$S_m = S_{mo}\rho \quad (12)$$

where  $S_{mo}$  is the field strength at the inner surface of the outer wall and is given by  $B_o/\mu_o r_o$ . The radial velocity of the biological cell directed toward the outer wall is then a function of reduced radial distance  $\rho$  from the axis, given by

$$u_m(\rho) = m_m S_{mo}\rho \quad (13)$$

If we assume that the axial component of cell velocity corresponds to the local fluid velocity and the radial component is given by the simple equation above, then cell trajectories, and hence the separation behavior of the cell sorter, may be predicted.

**Cell Trajectory.** The radial component of the cell trajectory,  $dr/dt$ , is equal to the field-induced velocity and is given by eq 13. The axial component of the cell trajectory,  $dz/dt$ , is assumed to

correspond to local fluid velocity in the annulus. This is given by<sup>24</sup>

$$v(\rho) = \frac{2\langle v \rangle}{A_1} (1 - \rho^2 + A_2 \ln \rho) \quad (14)$$

where  $\langle v \rangle$  is the mean fluid velocity along the length of the annulus and  $A_1$  and  $A_2$  are functions of the ratio of inner to outer radii,  $r_i/r_o = \rho_i$ , of the annulus:

$$A_1 = (1 + \rho_i^2 - A_2) \quad (15)$$

$$A_2 = (1 - \rho_i^2) / \ln(1/\rho_i) \quad (16)$$

(Note that  $A_2$ , as defined above, is positive over the range  $0 < \rho_i < 1$  and this definition differs from that given in our earlier publication<sup>14</sup> by a factor of  $-1$ .) Cell trajectory is then described by the integral equation

$$\int_0^z dz = \int_{\rho_1}^{\rho} \frac{v(\rho)}{u_m(\rho)} d\rho \quad (17)$$

where  $\rho_1$  corresponds to the initial radial position at  $z = 0$  and  $\rho$  corresponds to the radial position at arbitrary distance  $z$  from the inlet splitter. In this work, we do not consider the small region where the flows from inlets a and a' merge or the region close to the outlet stream splitter where the flows diverge. Carrying out the integration, we obtain the equation

$$z = \frac{r_o \langle v \rangle}{2A_1 m_m S_{mo}} [4 \ln \rho - 2\rho^2 + 2A_2 (\ln \rho)^2]_{\rho_1}^{\rho} \quad (18)$$

The volumetric flow rate  $\dot{V}$  along the annulus is given by

$$\dot{V} = \pi r_o^2 \langle v \rangle (1 - \rho_i^2) \quad (19)$$

We may therefore substitute for  $\langle v \rangle$  in eq 18 and rearrange the result to the form

$$2\pi r_o m_m S_{mo} A_1 (1 - \rho_i^2) z = \dot{V} I_1[\rho_1, \rho] \quad (20)$$

in which

$$I_1[\rho_1, \rho] = [4 \ln \rho - 2\rho^2 + 2A_2 (\ln \rho)^2]_{\rho_1}^{\rho} \quad (21)$$

Trajectories are determined by solving eq 20 for  $z$ , for a series of discrete radial positions  $\rho$  and initial positions  $\rho_1$ . Examples of such trajectory calculations have been presented earlier.<sup>14,25</sup> It is possible for a cell to be driven from its initial radial position  $\rho_1$  to the surface of the outer wall of the annulus, at  $\rho = 1$ , before it has time to be carried along the full length of the annulus. If this is not the case, its final radial position  $\rho_2$ , at a point just prior to

(21) Chalmers, J. J.; Zhao, Y.; Nakamura, M.; Melnik, K.; Lasky, L.; Moore, L. R.; Zborowski, M. *J. Magn. Magn. Mater.* **1999**, *194*, 231–241.

(22) Chalmers, J. J.; Haam, S.; Zhao, Y.; McCloskey, K.; Moore, L. R.; Zborowski, M.; Williams, P. S. *Biotechnol. Bioeng.*, in press.

(23) Dawson, P. H. *Quadrupole Mass Spectrometry and Its Applications*; Elsevier Scientific Publishing Co.: New York, 1976.

(24) Bird, R. B.; Stewart, W. E.; Lightfoot, E. N. *Transport Phenomena*; John Wiley & Sons: New York, 1960; pp 51–54.

(25) Williams, P. S. *Sep. Sci. Technol.* **1994**, *29*, 11–45.

the division of the carrier fluid by the outlet stream splitter, may be determined by numerical solution of the equation

$$2\pi r_o m_m S_{mo} A_1 (1 - \rho_i^2) L = \dot{V} I_1[\rho_1, \rho_2] \quad (22)$$

We note that the simplifications<sup>2</sup> that were applicable to the parallel-plate SPLIT system, in which the transverse component to particle velocity and the channel breadth are constant across the channel thickness, are not applicable to the annular magnetic system. We cannot reduce the radial migration of a population of cells of some discrete mobility to a migration across a fixed fraction of volumetric flow rate  $\Delta \dot{V}$ . In the case of the annular system, the quantity  $\Delta \dot{V}$  would be a function of initial radial position  $\rho_1$  in addition to the cell mobility and the system parameters  $B_o$ ,  $L$ ,  $\rho_i$ , and  $\dot{V}$ .

**Positions of Splitting Surfaces.** In a perfectly constructed annular system, the splitting surfaces would be cylindrical and concentric with the walls of the channel. In the present work, we shall assume the system is indeed perfectly constructed. The volumetric flow rate of the fluid within the cylindrical inlet splitting surface (ISS) (i.e., between the inner wall and the ISS) must correspond to  $\dot{V}(a')$ , the flow rate at inlet  $a'$ . If the radius of the inlet splitting surface is represented by  $r_{ISS}$ , then we have

$$\dot{V}(a') = \int_{r_i}^{r_{ISS}} 2\pi r v(r) dr \quad (23)$$

Replacing the variable of integration with  $\rho$ , substituting for the velocity profile using eq 14, and integrating, we obtain the result

$$\dot{V}(a') = \frac{\pi r_o^2 \langle v \rangle}{A_1} I_2[\rho_i, \rho_{ISS}] \quad (24)$$

where  $I_2[\rho_i, \rho_{ISS}]$  represents the result of an integration and is given by

$$I_2[\rho_i, \rho_{ISS}] = [2\rho^2 - \rho^4 + 2A_2\rho^2 \ln \rho - A_2\rho^2]_{\rho_i}^{\rho_{ISS}} \quad (25)$$

The total flow rate in the annulus must correspond to an integration of flow velocity over the full area of cross section from  $r_i$  to  $r_o$  or from  $\rho_i$  to  $\rho = 1$ . The result of course reduces to eq 19. Dividing eq 24 by  $\dot{V}$  yields the equation

$$\frac{\dot{V}(a')}{\dot{V}} = \frac{I_2[\rho_i, \rho_{ISS}]}{I_2[\rho_i, 1]} = \frac{I_2[\rho_i, \rho_{ISS}]}{A_1(1 - \rho_i^2)} \quad (26)$$

A similar consideration of the fluid flow within the outlet splitting surface (OSS) results in

$$\frac{\dot{V}(a)}{\dot{V}} = \frac{I_2[\rho_i, \rho_{OSS}]}{I_2[\rho_i, 1]} = \frac{I_2[\rho_i, \rho_{OSS}]}{A_1(1 - \rho_i^2)} \quad (27)$$

**Critical Cell Mobilities.** It was mentioned earlier that, in the case of the annular system, it is not possible to employ some of the simplifications applicable to the parallel-plate SPLIT system.

Cells of a given mobility do not migrate across a fixed fraction of channel flow that is independent of their initial transverse positions. However, it is possible to associate particular cell mobilities with migration across specific intervals of the annular thickness. Consider, for the moment, that inlet and outlet flow rates ( $\dot{V}(a')$ ,  $\dot{V}(b')$ ,  $\dot{V}(a)$ , and  $\dot{V}(b)$ ) for a given system are fixed, which in turn fixes both  $\rho_{ISS}$  and  $\rho_{OSS}$ . Now consider a cell that is located initially at the ISS. Suppose this cell, having a critical mobility  $m_0$  (we omit the subscript  $m$  for the critical mobilities for reasons of simplicity), is driven just to the OSS in the time it is carried along the full length of the system. It follows that cells having mobilities lower than  $m_0$ , and initially located at any  $\rho \leq \rho_{ISS}$  (i.e., anywhere in the sample lamina), cannot be driven beyond  $\rho_{OSS}$  and therefore cannot exit at outlet  $b$ . All cells having mobilities less than the critical mobility of  $m_0$  must therefore exit at outlet  $a$ . The fraction of cells having mobility less than  $m_0$  that exit outlet  $b$  must therefore be zero. We may state that, for  $m_m < m_0$ , we expect  $F_b = 0$ , where  $F_b$  represents the fraction of cells of a given mobility that exit at outlet  $b$ . From eq 22, we see that

$$m_0 = \frac{\dot{V}}{2\pi r_o L S_{mo}} \frac{I_1[\rho_{ISS}, \rho_{OSS}]}{A_1(1 - \rho_i^2)} \quad (28)$$

We can consider a second critical cell mobility  $m_1$  corresponding to that for a cell that is driven from the inner wall of the annulus just to the OSS in the time it is carried along the length of the system. If we assume for the moment that all cells driven beyond the OSS exit at outlet  $b$ , then for  $m_m > m_1$ , we expect  $F_b = 1$ . Again, a consideration of eq 22 shows that

$$m_1 = \frac{\dot{V}}{2\pi r_o L S_{mo}} \frac{I_1[\rho_i, \rho_{OSS}]}{A_1(1 - \rho_i^2)} \quad (29)$$

In the separation of biological cells, it is generally essential that one or both of the fractions collected remain largely viable. An encounter with the outer wall of the annulus, or even with the higher fluid shear rates near the wall, may damage cells. It is therefore of interest to predict the fraction of cells, as a function of mobility, that have time to migrate this far. Cells that do migrate to the outer wall may succumb to various fates, as will be discussed below. However, we can safely say that cells that do not have time to migrate to the outer wall will be carried in suspension to the system outlets. We can define a critical mobility  $m_2$  corresponding to a cell that migrates from the ISS just to the outer wall of the annulus as it passes along the system. No cells starting from within the sample lamina and having a lower mobility than  $m_2$  will have time to migrate as far as the outer wall. If  $F_w$  represents the fraction of cells of a given mobility that have time to migrate as far as the outer wall, then we can say that, for  $m_m < m_2$ ,  $F_w = 0$ . From eq 22, we obtain the following equation for  $m_2$ :

$$m_2 = \frac{\dot{V}}{2\pi r_o L S_{mo}} \frac{I_1[\rho_{ISS}, 1]}{A_1(1 - \rho_i^2)} \quad (30)$$

Finally, a critical cell mobility  $m_3$  may be assigned to a cell that migrates from the inner wall to the outer wall during its

passage through the system. All cells having higher mobility than  $m_3$  therefore have sufficient time to be driven as far as the outer wall. We then have  $F_w = 1$  for  $m_m > m_3$ . The mobility  $m_3$  is given by the equation

$$m_3 = \frac{\dot{V}}{2\pi r_o L S_{mo}} \frac{I_1[\rho_i, 1]}{A_1(1 - \rho_i^2)} = \frac{\dot{V}}{\pi r_o L S_{mo} A_2} \quad (31)$$

The rather simple result on the right, above, is obtained via an expansion of  $I_1[\rho_i, 1]$ .

From the definition of  $I_1[\rho_i, \rho_2]$  given by eq 21, it may be shown that

$$I_1[\rho_i, 1] = I_1[\rho_{ISS}, 1] + I_1[\rho_i, \rho_{OSS}] - I_1[\rho_{ISS}, \rho_{OSS}] \quad (32)$$

and it follows that  $m_3$  is dependent on  $m_0$ ,  $m_1$ , and  $m_2$  according to the equation

$$m_3 = m_2 + m_1 - m_0 \quad (33)$$

Consider now those cells that migrate as far as the outer wall. As a cell approaches the wall, the force driving it to the wall tends to be opposed by hydrodynamic lift forces (see refs 26–30). Depending on the size of the cell and the fluid shear rate close to the wall, these may be sufficiently strong that the cell is prevented from impacting the surface. The cell would be carried in suspension to outlet b, albeit under higher shear conditions than those cells which remain in the main body of the flow. The fate of cells that migrate as far as the outer wall is therefore expected to depend on cell properties and flow conditions. At present, only experiment can determine the outcome. The force with which a cell is driven toward the outer wall is proportional to the product  $m_m f$ . It may be found that, under given flow conditions, cells of a particular type, having a mobility below some critical level (e.g.,  $m_4$ ), are prevented from impacting the wall by the action of opposing hydrodynamic lift forces. In the case that  $m_4 > m_3 > m_2$ , this effect may extend the range of mobilities (up to  $m_4$ ) for viable cells collected at outlet b. Those cells having mobility greater than  $m_4$  may be retained on the surface of the outer wall. We can designate the fraction of cells that are retained by  $F_r$ , and according to our simple model, we expect  $F_r = 1$  for  $m_m > m_4$ . We shall define the fraction  $F_w$  to refer to cells that are driven as far as the outer wall but remain mobile. These cells are likely to remain viable. It has been found that some of the retained cells also remain viable and that they may be flushed from the system after removing the magnetic field.

The various cell fractions  $F_a$ ,  $F_b$ ,  $F_w$ , and  $F_r$  are functions of cell mobility. For any particular mobility, their sum must be equal to unity. They may therefore be represented by their contribution to the area beneath the constant unit function as shown in Figure

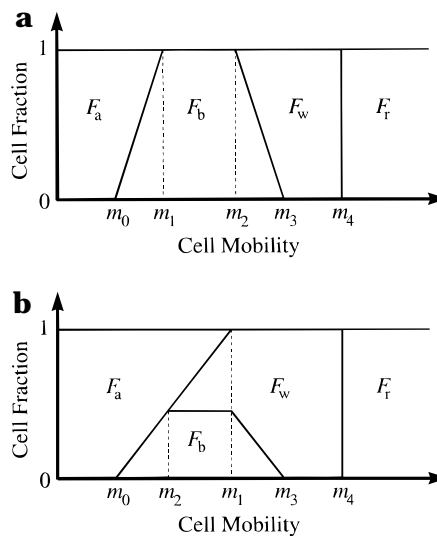


Figure 2. Fate of cells as a function of magnetophoretic mobility:  $F_a$ , fraction exiting outlet a;  $F_b$ , fraction exiting outlet b;  $F_w$ , fraction migrating to the outer wall but still carried to outlet b;  $F_r$ , fraction being retained on the outer wall. Key: (a) example where  $m_0 < m_1 < m_2 < m_3 < m_4$ ; (b) example where  $m_0 < m_2 < m_1 < m_3 < m_4$ .

2. Figure 2a shows the simplest situation where  $m_0 < m_1 < m_2 < m_3 < m_4$ . Note that the boundaries between contributing areas have been approximated by straight lines. For the case shown in Figure 2a, 100% of the cells exhibiting mobilities between  $m_1$  and  $m_2$  are carried in suspension to outlet b. A gradually decreasing fraction of cells having mobilities up to  $m_3$  are also carried in suspension to outlet b. This occurs while an increasing fraction between  $m_2$  and  $m_3$  and all cells up to  $m_4$  are carried along the wall to outlet b with the aid of hydrodynamic lift forces. Cells with mobility greater than  $m_4$  are retained on the outer wall of the annulus but may remain viable. Under certain conditions, it is possible for  $m_2$  to be smaller than  $m_1$ . Consider a population of cells having a discrete mobility  $m_m$  introduced to the system under such conditions and suppose that  $m_2 < m_m < m_1$ . A fraction of the cells initially located close to the ISS will have time to migrate to the outer wall while a fraction initially located close to the inner wall will not have time to migrate beyond the OSS and exit outlet b. It follows that some of the cells will exit at outlet a and some will exit at outlet b. Some will migrate as far as the outer wall where they may or may not be adsorbed and/or damaged, as discussed earlier. An example of such a situation is shown in Figure 2b, where  $m_0 < m_2 < m_1 < m_3 < m_4$ . For the particular example shown,  $m_1 < m_3 < m_4$  so that those cells which are carried to the outer wall remain mobile and exit at outlet b. The critical mobility  $m_4$  is not a function of the other critical mobilities. It may be found from experiment that  $m_4 < m_2$ , in which case all cells that are carried to the outer wall are retained in the system. It will be shown below that such a situation may be avoided with a suitable selection of flow rate regime.

**Resolving Power.** Resolving power for SPLITT systems was defined by Giddings<sup>31</sup> as  $m_1/\Delta m$  where  $\Delta m = m_1 - m_0$ , or alternatively as  $\bar{m}/\Delta m$  where  $\bar{m} = (m_0 + m_1)/2$ . It is a measure of how sharply resolved the cell populations collected at outlets a

(26) Ho, B. P.; Leal, L. G. *J. Fluid Mech.* **1974**, *65*, 365–400.  
 (27) Vasseur, P.; Cox, R. G. *J. Fluid Mech.* **1976**, *78*, 385–413.  
 (28) Williams, P. S.; Koch, T.; Giddings, J. C. *Chem. Eng. Commun.* **1992**, *111*, 121–147.  
 (29) Williams, P. S.; Lee, S.; Giddings, J. C. *Chem. Eng. Commun.*, **1994**, *130*, 143–166.  
 (30) Williams, P. S.; Moon, M. H.; Xu, Y.; Giddings, J. C. *Chem. Eng. Sci.*, **1996**, *51*, 4477–4488.

(31) Giddings, J. C. *Sep. Sci. Technol.* **1992**, *27*, 1489–1504.

and b are expected to be. From eqs 28 and 29 it may be shown that

$$\frac{m_1}{\Delta m} = \frac{I_1[\rho_i, \rho_{\text{OSS}}]}{I_1[\rho_i, \rho_{\text{ISS}}]} \quad (34)$$

Also, if we represent the ratio  $m_1/m_0$  by  $R_{10}$ , we see that

$$\frac{m_1}{\Delta m} = \frac{R_{10}}{R_{10} - 1} \quad (35)$$

**Throughput.** With a flow rate regime correctly set up to isolate or enrich some range of mobility of interest, the system throughput may be defined as the number of cells introduced to the system and sorted per unit time. This corresponds to the product of  $\dot{V}(a')$ , the sample feed streamflow rate, and  $C$ , the number concentration of cells in the feed stream. We may rearrange eq 29 to obtain the following expression for  $\dot{V}$ :

$$\dot{V} = 2\pi r_o L S_{\text{mo}} m_1 \frac{A_1(1 - \rho_i^2)}{I_1[\rho_i, \rho_{\text{OSS}}]} \quad (36)$$

From eqs 26 and 36, we see that

$$\text{TP} = C\dot{V}(a') = 2\pi r_o L S_{\text{mo}} m_1 C \frac{I_2[\rho_i, \rho_{\text{ISS}}]}{I_1[\rho_i, \rho_{\text{OSS}}]} \quad (37)$$

Taking eqs 11 and 34 into account, this may be written in the form

$$\text{TP} = 2\pi L \frac{B_o^2}{\mu_0} m_1 C \frac{I_2[\rho_i, \rho_{\text{ISS}}]}{I_1[\rho_i, \rho_{\text{ISS}}]} \frac{1}{m_1/\Delta m} \quad (38)$$

The latter form shows that throughput is proportional to channel length, field strength, and absolute mobilities and inversely proportional to resolving power. We shall consider the factors influencing system throughput in more detail elsewhere.

**Dilution Factor.** If we assume that the flow regime has been set up to collect viable cells of interest at outlet b (and this may require that these cells not migrate to the outer wall), it immediately follows that the dilution factor for these cells is given by

$$\text{DF} = \frac{\dot{V}(b)}{\dot{V}(a')} = \frac{I_2[\rho_{\text{OSS}}, 1]}{I_2[\rho_i, \rho_{\text{ISS}}]} \quad (39)$$

#### SETUP OF REQUIRED FLOW RATE REGIME

In the following examples we consider situations where the cells of interest are to be collected only at outlet b. The methods would require modification if the product was to be collected at outlet a. The approach to setup of flow rates may also depend on the nature of the sample. We shall consider some different situations. If a cell type of interest was found to be particularly fragile and sensitive to any approach to a bounding wall, then it would be necessary to ensure that the sorting took place without

allowing any of these cells to migrate to the outer wall. This could be accomplished by arranging for critical mobilities  $m_1$  and  $m_2$  to bound the mobility range of these cells. This situation is the first to be considered below. For more robust cell types, the approach to the outer wall may not present a viability problem. If cells that approach the wall are also found to remain mobile, then we are free to modify the dilution factor to some extent. This corresponds to the second situation considered below. Finally, it may be found that, depending on the flow rate  $\dot{V}$ , some cells are retained on the outer wall. It would be expected that the critical mobility  $m_4$  corresponding to the commencement of cell retention would be a function of  $\dot{V}$ . This effect would have to be taken into account in the setup of flow rates and is also considered below.

**Cells of Interest Prevented from Approaching the Outer Wall.** In the previous section, it was shown how certain critical cell mobilities are associated with a given flow rate regime. In practice, it will usually be the case that cells of some known range of mobility require isolation or enrichment. The critical mobilities that are to bound the range of interest are therefore known, and the flow regime consistent with these critical mobilities is required. An approach to determining a suitable flow rate regime is described below.

The required critical mobilities  $m_1$  and  $m_2$  may be set to include the range of mobility for the cells of interest. A required resolving power  $m_1/\Delta m$  may also be set, which in turn fixes  $m_0$  and  $m_3$ . The ratio  $m_1/m_0$  was earlier represented by  $R_{10}$  in relation to eq 35. From eqs 28 and 29 we have

$$R_{10} = \frac{m_1}{m_0} = \frac{I_1[\rho_i, \rho_{\text{OSS}}]}{I_1[\rho_{\text{ISS}}, \rho_{\text{OSS}}]} \quad (40)$$

which may be shown to be consistent with eq 35. Suppose the ratio  $m_2/m_1$  is represented by  $R_{21}$ . From eqs 29 and 30, it may be shown that

$$R_{21} = \frac{m_2}{m_1} = \frac{I_1[\rho_{\text{ISS}}, 1]}{I_1[\rho_i, \rho_{\text{OSS}}]} \quad (41)$$

The required value for  $R_{21}$  is determined by the relative range of mobility exhibited by the cell type of interest. Typically,  $R_{21}$  will allow for a relative range of mobility of between 1 and 2 orders of magnitude. The function  $I_1[\rho_1, \rho_2]$ , defined by eq 21, represents the result of an integration, where  $\rho_1$  and  $\rho_2$  are the initial and final reduced radial positions for a cell as it is carried through the system. We may write this in the alternative form

$$I_1[\rho_1, \rho_2] = f_1(\rho_2) - f_1(\rho_1) \quad (42)$$

where

$$f_1(\rho) = 4 \ln \rho - 2\rho^2 + 2A_2(\ln \rho)^2 \quad (43)$$

Substituting for  $I_1[\rho_1, \rho_2]$  in eqs 40 and 41 and solving the two simultaneous equations for  $f_1(\rho_{\text{ISS}})$  and  $f_1(\rho_{\text{OSS}})$ , we obtain the solutions

$$f_1(\rho_{\text{ISS}}) = \frac{R_{21}R_{10}f_1(\rho_i) + (R_{10} - 1)f_1(1)}{R_{21}R_{10} + R_{10} - 1} \quad (44)$$

$$f_1(\rho_{\text{OSS}}) = \frac{(R_{21}R_{10} - 1)f_1(\rho_i) + R_{10}f_1(1)}{R_{21}R_{10} + R_{10} - 1} \quad (45)$$

for which we note that  $f_1(1) = -2$ . These equations require numerical solution for  $\rho_{\text{ISS}}$  and  $\rho_{\text{OSS}}$ . Once these are obtained, we have sufficient information to calculate flow rate ratios at inlets and outlets via eqs 26 and 27. The required absolute flow rates are established with consideration of an absolute mobility. Taking  $m_1$  as the reference mobility, the total flow rate  $\dot{V}$  is given by eq 36. We could alternatively consider the value for mobility  $m_3$  in conjunction with eq 31 to yield the somewhat simpler result

$$\dot{V} = \pi r_0 L S_{\text{mo}} m_3 A_2 \quad (46)$$

The individual flow rates at the inlets and outlets are then determined using eqs 26 and 27, taking into account that  $\dot{V}(b) = \dot{V} - \dot{V}(a)$  and  $\dot{V}(b) = \dot{V} - \dot{V}(a)$ .

We shall now consider a specific example. Suppose the system parameters are as follows:  $r_0 = 9.5$  mm,  $\rho_i = 0.75$ ,  $L = 15$  cm, and  $B_0 = 1.2$  T. Also,  $\mu_0$  is a constant equal to  $4\pi \times 10^{-7}$  T m/A. Then suppose we are interested in collecting cells covering a single order of magnitude in mobility from  $m_1 = 1 \times 10^{-13}$  m<sup>3</sup>/(T A s) to  $m_2 = 1 \times 10^{-12}$  m<sup>3</sup>/(T A s) at outlet b and suppose we set the required resolving power  $m_1/\Delta m$  to 2. It follows that  $m_0 = 5 \times 10^{-14}$  m<sup>3</sup>/(T A s) and  $m_3 = 1.05 \times 10^{-12}$  m<sup>3</sup>/(T A s). Solving eqs 44 and 45 with  $R_{10} = 2$  and  $R_{21} = 10$ , we obtain  $\rho_{\text{ISS}} = 0.780$  and  $\rho_{\text{OSS}} = 0.794$ . From these values we may calculate the transverse transport lamina thickness  $\Delta r = r_{\text{OSS}} - r_{\text{ISS}}$  to be 133  $\mu\text{m}$ . The required total flow rate  $\dot{V}$  is calculated using eq 46 to be  $8.62 \times 10^{-7}$  m<sup>3</sup>/s, or 51.7 mL/min. From eqs 26 and 27 we obtain the required flow rates  $\dot{V}(a) = 1.89$  mL/min and  $\dot{V}(b) = 3.93$  mL/min. For a sample feed stream concentration of  $10^8$  cells/mL, the system throughput TP =  $1.89 \times 10^8$  cells/min, or  $1.1 \times 10^{10}$  cells/h. Finally, we may calculate the dilution factor for these cells to be 25.3, and it is likely that some concentration step would be required following the sorting procedure. Note that these conditions are presented only for the purposes of illustration and are not representative of a fully optimized system.

The approach described is only one of several possible approaches. Any two of the four eqs 37, 39, 40, and 41 may be solved simultaneously for  $\rho_{\text{ISS}}$  and  $\rho_{\text{OSS}}$ . For example, a mobility range of interest may be specified along with some required system throughput (eqs 41 and 37 would then require solution). Of course, depending on the specified requirements, both dilution factor and resolving power may be unacceptably compromised. However, all four equations may be considered in order to obtain the best overall set of conditions.

**Cells of Interest Allowed To Approach the Outer Wall.** In this case, we assume that cells remain mobile when they migrate to the outer wall and are carried to outlet b. We are therefore simply concerned that  $m_1$  corresponds to the lowest mobility for the cells of interest, and we do not have to relate  $m_2$  to the upper end of the mobility range of interest. All cells of higher mobility than  $m_1$  will be carried beyond the OSS and therefore to outlet b.

As before, we can set a required resolving power of  $m_1/\Delta m$ , which fixes  $m_0$ . Provided cells reaching the outer wall remain mobile, the outlet splitting surface may be placed arbitrarily close to the outer wall. This means that we have complete control over the dilution factor. In principle, it would be possible to isolate the cell fraction of interest while at the same time obtaining an increased concentration of this fraction. We can approach the setup of flow rates as follows. Solutions may be obtained for  $\rho_{\text{ISS}}$  and  $\rho_{\text{OSS}}$  by simultaneously solving eqs 39 (with some desired dilution factor) and 40 (with  $R_{10}$  consistent with the required resolving power). The total flow rate  $\dot{V}$  is then determined using eq 36 (since the mobility  $m_3$  is, in this case, irrelevant); the individual flow rates are determined as before.

Suppose system parameters, the required resolving power, and the cell mobility range of interest are the same as for the example above. This time, however, we shall require a dilution factor of only 2. The solution for the placement of splitting surfaces results in  $\rho_{\text{ISS}} = 0.833$  and  $\rho_{\text{OSS}} = 0.881$ . From these we calculate a transport lamina thickness  $\Delta r$  of 456  $\mu\text{m}$ . The total required flow rate  $\dot{V}$  is calculated to be  $1.44 \times 10^{-7}$  m<sup>3</sup>/s, or 8.62 mL/min. From eqs 26 and 27 we obtain the required flow rates  $\dot{V}(a) = 2.08$  mL/min and  $\dot{V}(b) = 4.46$  mL/min. Note that it follows that  $\dot{V}(b) = 4.16$  mL/min, which is consistent with the dilution factor of 2. For a sample feed stream concentration of  $10^8$  cells/mL, the system throughput TP =  $2.08 \times 10^8$  cells/min, or  $1.2 \times 10^{10}$  cells/h. Compared to the previous calculated conditions, we see that the dilution factor is of course greatly reduced from 25.3 to 2, as required. The transport lamina thickness is also increased from 133 to 456  $\mu\text{m}$  and is positioned more toward the center of the annulus. This is likely to be a great practical advantage as the sorting efficiency should be more forgiving of small imperfections in both the system construction and the implementation of flow rates. (These aspects will be the topic of another study.) The advantages are obtained along with a slight increase in  $\dot{V}(a)$  and system throughput. For the selected conditions, we calculate values for  $m_2$  and  $m_3$  of  $1.25 \times 10^{-13}$  and  $1.75 \times 10^{-13}$  m<sup>3</sup>/(T A s), respectively. The assumed mobility range of interest extends up to  $1 \times 10^{-12}$  m<sup>3</sup>/(T A s), which is considerably higher than the  $m_2$  and  $m_3$  for the selected conditions. The advantages of the selected conditions over those found previously (for  $m_2 = 1 \times 10^{-12}$  m<sup>3</sup>/(T A s)) are clear, particularly with regard to dilution of samples. We are not concerned here with a full optimization of the system, but it is apparent that there would be advantages in chemically treating the outer wall to reduce the tendency for cell adsorption. This would allow for selection of more attractive conditions, such as those calculated here.

Again, the approach described is just one of, in this case, three possible initial approaches. Since it is assumed that the value for  $m_2$  does not put a restriction on the cells collected at outlet b, eq 41 is not taken into account in determining the required conditions. We are left with selecting two out of the three eqs 37, 39, and 40 to solve for  $\rho_{\text{ISS}}$  and  $\rho_{\text{OSS}}$ . For the example shown, eqs 39 and 40 were solved.

**Cells of Interest Allowed To Approach the Outer Wall—Provided They Remain Mobile.** The case just described above amounts to an ideal situation. In practice, cell retention on the outer wall is likely to occur under some conditions. The critical cell mobility  $m_4$  at which retention commences is expected to be

some function of total flow rate  $\dot{V}$  for a given system geometry. The relationship, which would probably be dependent on cell type, would have to be determined from experiment. Once the relationship is known for the cell type of interest, it would be possible to obtain the  $\dot{V}$  required to equate  $m_4$  with the upper end of the mobility range of interest. Equation 36 may then be solved numerically for  $\rho_{\text{OSS}}$ . If a certain level of resolving power is required, eq 40 may then be solved numerically for  $\rho_{\text{ISS}}$ . The individual flow rates are then obtainable using eqs 26 and 27, as before. The resulting flow rate conditions will give the lowest dilution factor consistent with mobility for the cells of interest and the required resolving power.

Suppose we continue with the example discussed above but find that, to obtain  $m_4 = 1 \times 10^{-12} \text{ m}^3/(\text{T A s})$ , we need to raise  $\dot{V}$  to 12.0 mL/min. Solution of eq 36 yields a value of 0.854 for  $\rho_{\text{OSS}}$ . For a required resolving power of 2, eq 40 then yields 0.818 for  $\rho_{\text{ISS}}$ . Compared to the conditions selected when there was no restriction placed on  $\dot{V}$ , we see that transport lamina thickness is reduced to 342  $\mu\text{m}$  and the transport lamina is displaced slightly toward the inner wall of the annulus. The dilution factor is also somewhat increased to 3.77, while critical mobilities  $m_2$  and  $m_3$  rise to  $1.94 \times 10^{-13}$  and  $2.44 \times 10^{-13} \text{ m}^3/(\text{T A s})$ , respectively. It is apparent that there must be some compromise in conditions in order to ensure mobility of the cells of interest. The conditions remain far more desirable, from a practical standpoint, than those obtained for the requirement that none of the cells of interest approach the outer wall.

In this case, there are again three possible initial approaches. The simultaneous equations to be solved for  $\rho_{\text{ISS}}$  and  $\rho_{\text{OSS}}$  must include eq 36 with one of eqs 37, 39, and 40. It is simply a matter of selecting the most important factor: system throughput, dilution factor, or resolving power. Following the initial solution, a compromise may of course be necessary.

#### EMPIRICALLY OPTIMIZED FLOW RATE REGIMES: COMPARISON WITH THEORY

It was mentioned earlier that several studies of cell sorting using the quadrupole sorter have already been presented.<sup>14–19</sup> In the absence of magnetophoretic mobility data for the labeled cells, an empirical approach to setup of flow rate conditions was necessarily taken. However, some preliminary measurements of labeled cell mobilities have recently become available<sup>21,22</sup> and it is now possible to quantitatively evaluate some of these empirically selected conditions using the theory presented in the present work. We need only select sorting and mobility studies having labeled cell types in common. One of the sorting studies (that of Sun et al.<sup>16</sup>) included enrichment of labeled CD8 and CD45 human lymphocytes and depletion of unlabeled cells from labeled CD45 lymphocytes. The cells were labeled with a primary mouse anti-human CDx monoclonal antibody (mAb) conjugated to fluorescein isothiocyanate (FITC) and a secondary rat anti-mouse polyclonal antibody (pAb) conjugated to an iron–dextran colloid (MACS microbeads of Miltenyi Biotec GmbH, Bergisch Gladbach, Germany). The FITC conjugate was included to allow the sorted fractions to be analyzed by fluorescence-activated cell scanning (FACS). Chalmers et al.<sup>21</sup> recently published magnetophoretic mobility histograms for similarly labeled CD8 and CD45 human lymphocytes.

The quadrupole system used by Sun et al.<sup>16</sup> had the dimensions  $r_0 = 4.41 \text{ mm}$ ,  $r_1 = 2.38 \text{ mm}$ , and  $L = 76.2 \text{ mm}$ . The magnetic flux density at the pole tips was found to be 0.9 T, from which we may estimate  $B_0$  of 0.83 T at the outer wall radius  $r_0$  (assuming a tube wall thickness of 0.35 mm) and  $S_{\text{mo}}$  of  $1.2 \times 10^8 \text{ T A/m}^2$ . For enrichment of labeled CD8 cells, the following flow rates were set:  $\dot{V}(a') = 0.30 \text{ mL/min}$ ,  $\dot{V}(b') = 2.70 \text{ mL/min}$ ,  $\dot{V}(a) = 0.90 \text{ mL/min}$ , and  $\dot{V}(b) = 2.10 \text{ mL/min}$ . Solving eqs 26 and 27, we obtain  $\rho_{\text{ISS}} = 0.638$  and  $\rho_{\text{OSS}} = 0.718$ , respectively. From eqs 28–31 we calculate  $m_0 = 8.3 \times 10^{-14} \text{ m}^3/(\text{T A s})$ ,  $m_1 = 1.4 \times 10^{-13} \text{ m}^3/(\text{T A s})$ ,  $m_2 = 2.8 \times 10^{-13} \text{ m}^3/(\text{T A s})$ , and  $m_3 = 3.3 \times 10^{-13} \text{ m}^3/(\text{T A s})$ . The mobility histogram shown by Chalmers et al.<sup>21</sup> for similarly labeled CD8 cells shows a wide distribution from around  $10^{-15} - 10^{-12} \text{ m}^3/(\text{T A s})$ , with the majority falling between  $10^{-14}$  and  $10^{-12} \text{ m}^3/(\text{T A s})$ . However, the lower range of mobility was said to be subject to uncertainty due to residual motion of the cells following sample input to the instrument. (The experiments were of a preliminary nature, and further improvements to the technique are expected.) The sorting experiments resulted in approximately a 2:1 distribution of labeled cells between the b and a outlet streams, respectively, with good total recovery (90% and 97% recovery for the two experiments reported). If we accept that cells having mobility between  $3 \times 10^{-13}$  and  $1 \times 10^{-12} \text{ m}^3/(\text{T A s})$  may have been driven to the outer wall but remained mobile (as discussed earlier), then the agreement between theory and experiment appears to be remarkably good. Certainly, the critical mobilities  $m_0$  and  $m_1$  for the selected conditions are consistent with a selective enrichment of the more mobile of the labeled CD8 cells.

For the depletion of unlabeled cells (present at 6%) from labeled CD45 cells, flow rates were set as follows:  $\dot{V}(a') = 0.25 \text{ mL/min}$ ,  $\dot{V}(b') = 4.75 \text{ mL/min}$ ,  $\dot{V}(a) = 1.00 \text{ mL/min}$ , and  $\dot{V}(b) = 4.00 \text{ mL/min}$ . For these conditions, we calculate  $\rho_{\text{ISS}} = 0.608$ ,  $\rho_{\text{OSS}} = 0.682$ ,  $m_0 = 1.1 \times 10^{-13} \text{ m}^3/(\text{T A s})$ ,  $m_1 = 1.6 \times 10^{-13} \text{ m}^3/(\text{T A s})$ ,  $m_2 = 5.1 \times 10^{-13} \text{ m}^3/(\text{T A s})$ , and  $m_3 = 5.5 \times 10^{-13} \text{ m}^3/(\text{T A s})$ . The mobility histogram shown by Chalmers et al.<sup>21</sup> for similarly labeled CD45 cells shows a distribution from  $10^{-14}$  to  $10^{-12} \text{ m}^3/(\text{T A s})$ , with the majority falling between about  $5 \times 10^{-14}$  and  $5 \times 10^{-13} \text{ m}^3/(\text{T A s})$ , peaking quite sharply at  $2 \times 10^{-13} \text{ m}^3/(\text{T A s})$ . The selected flow conditions were apparently consistent with collection of the more mobile labeled CD45 cells at outlet b and with the less mobile labeled CD45 cells and the unlabeled cells directed to outlet a. Chalmers et al.<sup>21</sup> also presented a mobility histogram for an experiment where the primary antibody was omitted. The calculated  $m_0$  and  $m_1$  values are consistent with exclusion of effectively all such cells from collection at outlet b. The experiment of Sun et al.<sup>16</sup> in fact showed a 100% purity for the labeled CD45 cells collected at outlet b.

For enrichment of labeled CD45 cells (present in the feed stream at 3–5%), flow rates were set as follows:  $\dot{V}(a') = 0.12 \text{ mL/min}$ ,  $\dot{V}(b') = 3.88 \text{ mL/min}$ ,  $\dot{V}(a) = 0.80 \text{ mL/min}$ , and  $\dot{V}(b) = 3.20 \text{ mL/min}$ . For these conditions, we calculate  $\rho_{\text{ISS}} = 0.593$ ,  $\rho_{\text{OSS}} = 0.682$ ,  $m_0 = 1.1 \times 10^{-13} \text{ m}^3/(\text{T A s})$ ,  $m_1 = 1.3 \times 10^{-13} \text{ m}^3/(\text{T A s})$ ,  $m_2 = 4.2 \times 10^{-13} \text{ m}^3/(\text{T A s})$ , and  $m_3 = 4.4 \times 10^{-13} \text{ m}^3/(\text{T A s})$ . The selected conditions were again apparently consistent with collection of the more mobile labeled CD45 cells at outlet b.

Overall, we can say that there is a very encouraging agreement between theory and experiment.

## CONCLUSIONS

The consideration of certain specific cell trajectories within the quadrupole magnetic cell sorter has allowed the development of a strategy for optimizing the flow rate regime. It will now be possible to calculate the inlet and outlet flow rates necessary to achieve an isolation or purification of a given labeled cell type. This is an essential step toward the realization of the full potential of this cell-sorting technique.

## ACKNOWLEDGMENT

This work was supported by Grant NCI CA62349.

## LIST OF SYMBOLS

$A_c$	surface area of the biological cell
$A_1$	function of $\rho_1$ as defined by eq 16
$A_2$	function of $\rho_1$ as defined by eq 15
$B$	magnetic field intensity
$B_0$	magnetic field intensity at radius $r_0$
$C$	number concentration of cells
$d$	diameter of the spherical biological cell
DF	dilution factor
$f$	particle friction coefficient
$F_a$	fraction of cells of given mobility that exit at outlet a
$F_1$	force exerted on the magnetic label due to interaction with the magnetic field
$F_m$	force exerted on a particle due to interaction with the magnetic field
$F_b$	fraction of cells of given mobility that exit at outlet b
$F_r$	fraction of cells of given mobility that are retained on the outer wall
$F_w$	fraction of cells of given mobility that are driven to the outer wall of the annulus but remain mobile
$I_1[\rho_1, \rho_2]$	result of integration from $\rho_1$ to $\rho_2$ , as defined by eq 21
$I_2[\rho_1, \rho_2]$	result of integration from $\rho_1$ to $\rho_2$ , as defined by eq 25
$L$	channel length
$m_m$	magnetophoretic mobility
$m_0$	critical mobility such that, for $m_m < m_0$ , $F_a = 1$ and $F_b = 0$
$m_1$	critical mobility such that, for $m_m > m_1$ , $F_a = 0$ and $F_b = 1$
$m_2$	critical mobility such that, for $m_m < m_2$ , no cells have time to migrate to the outer wall
$m_3$	critical mobility such that, for $m_m > m_3$ , all cells have time to migrate to the outer wall

$m_4$	critical mobility such that, for $m_m > m_4$ , all cells are retained on the outer wall
$\Delta m$	$m_1 - m_0$
$r$	radial distance from the axis of the annulus
$r_{1SS}$	radius of the inlet splitting surface
$r_{OSS}$	radius of the outlet splitting surface
$\Delta r$	transport lamina thickness, $r_{OSS} - r_{1SS}$
$r_0$	radius of the inner surface of the outer wall of the annulus
$R_{10}$	$m_1/m_0$
$R_{21}$	$m_2/m_1$
$S_m$	magnetic field strength defined by eq 3
$S_{m0}$	magnetic field strength at radius $r_0$
TP	system throughput (number of cells per unit time)
$u_m$	velocity of the cell induced by interaction with the magnetic field
$v(\rho)$	fluid velocity as a function of $\rho$
$\langle v \rangle$	mean fluid velocity along the annulus
$V_m$	volume of a paramagnetic particle
$\dot{V}$	flow rate through the annulus
$\dot{V}(a)$	flow rate at outlet a
$\dot{V}(a')$	flow rate at inlet a'
$\dot{V}(b)$	flow rate at outlet b
$\dot{V}(b')$	flow rate at inlet b'
$z$	distance along the length of the annulus
$\alpha$	number of markers per unit area of cell surface
$\beta$	number of labels attached to each marker
$\Delta\chi$	magnetic susceptibility of a particle relative to that of the suspending medium
$\phi_1$	magnetic label–magnetic field interaction parameter
$\phi_m$	particle–magnetic field interaction parameter
$\eta$	fluid viscosity
$\mu_0$	magnetic permeability of free space
$\rho$	reduced radial distance, equal to $r/r_0$
$\rho_i$	reduced radius of the inner wall of the annulus, equal to $r_i/r_0$
$\rho_{1SS}$	reduced radius of the inlet splitting surface
$\rho_{OSS}$	reduced radius of the outlet splitting surface
$\rho_1$	initial reduced radial position of the cell
$\rho_2$	final reduced radial position of the cell

Received for review March 15, 1999. Accepted May 28, 1999.

AC990284+